Elsevier Editorial System(tm) for Scripta Materialia

Manuscript Draft

Manuscript Number: SMM-17-121R1

Title: Reverse austenite transformation behavior in a tempered martensite low-alloy steel studied using in situ neutron diffraction

Article Type: Regular article

Keywords: in situ neutron diffraction; tempered martensite; primary extinction; austenite memory; nucleation and growth.

Corresponding Author: Professor Yo Tomota, PhD

Corresponding Author's Institution: Ibaraki University

First Author: Yo Tomota, PhD

Order of Authors: Yo Tomota, PhD; Wu Gong, PhD; Sefanus Harjo, PhD; Tomoya Shinozaki, Master of Eng,

Abstract: The microstructure evolution during reverse transformation of a Cr-Ni-Mo steel consisting of tempered lath martensite and Cr carbide was examined using in situ neutron diffraction at high temperatures. The microstructural change from a reversed coarse-grained structure to a fine-grained polygonal structure by further annealing was monitored through a decrease in the diffraction intensity caused by primary extinction and the full width at half maximum. This result is different from that for a bainite steel, showing good coincidence with the observations using electron back scatter diffraction.

Reverse austenite transformation behavior in a tempered martensite low-alloy steel studied using *in situ* neutron diffraction

Y.Tomota[1*], W. Gong[2], S. Harjo[3] and T. Shinozaki[4]

[1] Research Center for Structure Materials, National Institute for Materials Science, 1-2-1 Sengen, Tsukuba, Ibaraki, 305-0047, Japan.

[2] Elements Strategy Initiative for Structural Materials, Kyoto University, Yoshida-honmachi, Sakyo-ku, Kyoto, 606-8501, Japan.

[3] J-PARC Center, Japan Atomic Energy Agency, 2-4 Shirane Shirakata, Tokai-mura, Naka-gun, Ibaraki, 319-1195, Japan.

[4] Steel Casting and Forging Division, Kobe Steel, Ltd., 2-3-1 Shinhama, Arai, Takasago, Hyogo, 676-8670, Japan.

*Corresponding author, E-mail: TOMOTA.Yo@nims.go.jp

Abstract

The microstructure evolution during reverse transformation of a Cr-Ni-Mo steel consisting of tempered lath martensite and Cr carbide was examined using *in situ* neutron diffraction at high temperatures. The microstructural change from a reversed coarse-grained structure to a fine-grained polygonal structure by further annealing was monitored through a decrease in the diffraction intensity caused by primary extinction and the full width at half maximum. This result is different from that for a bainite steel, showing good coincidence with the observations using electron back scatter diffraction.

Keywords

in situ neutron diffraction, tempered martensite, primary extinction, austenite memory, nucleation and growth.

Phase transformation from ferrite (α) to austenite (γ), *i.e.*, reverse transformation, has been utilized to refine the γ grain size in the steel production process. However, the γ grain size after the γ reversion in bainite or martensite steel sometimes becomes as large as that of the prior γ, which is called "γ memory" [1]. This reversed γ with coarse-grains changes to a fine-grained polygonal γ by further high-temperature annealing [2-4], which is similar to recrystallization. The mechanisms of such puzzling phenomena have been studied by many researchers [1,4-7], because it is a serious problem in industrial steel production. Shinozaki et al. have recently reviewed past studies and investigated the mechanism of the γ reversion behavior using *in situ* electron backscatter diffraction (EBSD) [8,9]. Their results on a tempered martensite steel [8,9] and a bainite steel [9] are summarized in Fig. 1, in which (a)-(d) show the tempered martensite steel containing mostly Cr carbides and a little cementite, while (e)-(h) show the bainite steel containing cementite particles. As observed, austenite grains nucleated during the reverse transformation are categorized into two types, A and B. The microstructures of Fig. 1(b) and (f) consist fully of austenite, in which examples of type B grains are indicated by red arrows. In Fig. 1(b), small number of type B equiaxed grains are scatted in the type A grains with lath shape (the matrix: see ref. 8 for more details). On the other hand, type B grains are dominantly observed in Fig. 1(f). For type A, γ grains nucleated at the lath boundaries with almost the same crystal orientation as that of the prior γ grain, whereas for type B, the γ grains nucleated at the prior γ grain boundaries or inside the prior γ grains with different crystal orientations. Type A grains are characterized by high kernel average misorientation (KAM) values, as seen in Fig. 1(c) and (g); on the other hand, the type B grains show very low KAM values (see red arrows in Fig. 1(c) and (g)). The most likely nucleation site inside the grain is the cementite particle. In the case of the tempered martensite steel, type A nucleation occurs predominantly because of the presence of a little cementite. Therefore, after the γ reverse transformation was completed, the prior γ grains were reconstructed by the growth of type A grains as seen in Fig. 1(b), which is called the γ memory phenomenon. As was discussed in ref. 8, this reverse transformation was not displacive (martensitic) but diffusional. Here, sub-boundaries remaining in such a reconstructed γ grain originally stemmed from the small-angle lath-boundaries of martensite (for details, see ref. 8). Hence, by heating to a higher temperature, type A grains were invaded and

eventually replaced by type B grains, resulting in a new fine-grained polygonal microstructure; this is similar to recrystallization behavior. These two types of γ nucleation are also observed in the bainite steel, as shown in Fig. 1(e)-(h). Different from the tempered martensite, type B grains nucleate predominantly in the bainite steel, so that a fine-grained γ structure appeared immediately after the completion of the γ reversion without showing γ memory. These are the main results recently obtained by surface observations with EBSD experiments [8,9], and this tentative conclusion is expected to be confirmed by evidence in the bulk, because the chemical compositions, particularly Mn and C, at the surface layer were suspected to change at elevated temperatures. Therefore, *in situ* neutron diffraction was employed in this study to monitor the γ reversion behavior of the tempered martensite steel using a bulk specimen.

The same steel as that used in Fig. 1(a)-(d) was used in this study. The chemical composition of the steel was 0.36C-0.22Si-0.79Mn-0.007P-0.003S-3.04Cr-1.46Ni-0.43Mo-0.1V-0.03Al (mass%) and balance Fe. The specimen was annealed at 1453 K for 3.6 ks, followed by quenching in water, and then the quenched specimen was tempered at 973 K for 54 ks with the aim of the precipitating the alloy carbides and the decomposing the retained γ . The Ac_1 and Ac_3 temperatures determined by dilatometry were 1003 K and 1088 K, respectively.

In situ neutron diffraction measurements were performed during the heat treatment using a time-of-flight (TOF) neutron diffractometer, TAKUMI at the Materials and Life Science Facility (MLF) in the Japan Proton Accelerator Research Complex (J-PARC). A cylindrical specimen with 8 mm in diameter and 30 mm in length was prepared. The neutron diffraction patterns in the axial and transverse directions were measured simultaneously using two detector banks having scattering angles of ±90°. The gauge volume was restricted to 5 × 5 × 5 mm^3 using an incident beam slit and radial collimators. The TAKUMI instrumental peak width, *i.e.*, wavelength resolution, was ~ 0.3% for the medium resolution mode used in this experiment. A thermocouple was welded on the specimen surface to measure and control the temperature. Heat treatment was conducted in vacuum to avoid oxidation. The specimen was heated at a heating rate of 1 K/s from 293 K (RT) to 993 K (before the start of reverse transformation) and held there for 1.2 ks, then heated up to 1048 K at 0.05 k/s and held there for 1.2 ks, then to 1193 K (after the

completion of γ reverse transformation), 1143 K, and finally 1223 K, in that order. The heat schedule is depicted in Fig. 2(a). The two-dimensional (2D) plots of the diffraction intensities of 111 γ, 200 γ, and 110 α peaks are presented in Fig. 2(b) as a function of the annealing time. As seen, it is found that the temperature range for α-to-γ transformation is almost consistent with that from Ac_1 to Ac_3 determined by dilatometry [8]. Here, both the diffraction peak intensity and full width at half maximum (FWHM) apparently decrease from 1143 K to 1223 K after becoming a single γ phase, which will be discussed later in detail. This corresponds to the EBSD results observed in Fig. 1 (b)-(d). Diffraction profiles (the axial direction) collected for 0.6 ks at the latter half of the isothermal holding at 1143 K and 1223 K are presented in Fig. 2(c). It is observed that the diffraction intensities of all the hkl peaks at 1223 K are smaller than those observed at 1143 K (see red arrows in the figure). Here the 200 peaks at the two temperatures were magnified in order to show the differences clearly; the peak shift due to thermal expansion, a large decrease in the maximum intensity and a small change of line profile broadening are found.

The detailed changes in the diffraction intensities and FWHMs of some hkl peaks obtained in the axial direction are shown in Fig. 3(a) and (b), respectively. The plotted values were obtained by time slicing of every 60 s for the event-mode recorded date and all the hkl peak intensities and FWHMs were normalized to the intensities and FWHMs at the beginning of holding the temperature at 1093 K, respectively. The peak intensities were found to drastically decrease upon heating from 1160 K to 1200 K (Fig. 3(a)). The lowest indexed peak of 111 (at the largest wavelength) shows the most significant drop in peak intensity (larger than 50%), while the drop in a higher indexed peak like 311 is small, in which the large scatters are due to its low absolute diffraction intensity. Similar drops in the hkl diffraction intensities were also observed in the results for the transverse direction. Therefore, such simultaneous drops in all peak intensities cannot be explained by a change in the texture. In the case of texture evolution, the diffraction intensities of some peaks would become stronger, whereas the others would become weaker. Kabra *et al*. observed a similar decrease in the neutron diffraction intensities of all the hkl peaks for the α-to-β transformation in a zirconium alloy and explained it by the effect of the primary extinction of the incident beam [10]. They have claimed that the increase in crystal perfection driven by thermal recovery causes a transition from the kinematic to the

dynamic theory of diffraction. The wavelength dependence observed in Fig. 3(a) can also be explained by the effect of primary extinction. Another possible origin of the decrease in all the peaks intensities is the effect of the Debye-Waller factor, but Kabra *et al*. have disregarded it because the amount of decreasing is estimated to be very small (approximately 5%) and its wavelength dependence is different from the primary extinction (the opposite trend) [10]. Hence, the results in Fig. 3(a) must be due to the primary extinction of the incident beam at elevated temperatures related to the growth of type B grains, which contain a very small dislocation density (small KAM value). It is concluded that the γ structure obtained by the growth of type A grains contain a high density of sub-boundary (dislocations array) that provides the driving force for the growth of type B grains. Since the density of nucleation site of type B grains is much smaller in the present tempered martensite steel compared with the bainite steel, the grain size of a polygonal γ structure achieved after the growth of type B grains would be relatively larger, as was found by comparing Fig. 1(d) with (h).

Contrary to the change in the diffraction intensity, the change in the relative FWHM shown in Fig. 3(b) is not so remarkable, although the drops are again observed over the same temperature range as in Fig. 3(a). The drop is the most remarkable for the 200 plane which corresponds to the lowest Young modulus in the 100 direction in a single fcc ferrous crystal [11]. That is, the wavelength dependence found in Fig. 3(b) is different from that observed in (a). Notably the microstructural change from 1143 K to 1223 K can be more remarkably found in the primary extinction than the FWHM related to dislocation density and crystallite size.

To obtain more quantitative insights on the microstructural features of the reversed γ, the convolutional multiple whole profile (CMWP) fitting [12,13] was performed for the single γ phase diffraction profiles obtained at 1093 K, 1143 K, and 1223 K. The dislocation density determined by the CMWP fitting for the 1143 K profile is 2.27×10^{14} m^{-2}, the dislocations arrangement parameter M is 0.30 and the dislocation character q is 1.8, which indicates that the edge component is dominant [14]. A small M value would suggest the low energy configuration of the dislocation structure, like dipole or polygonization, *i.e*., sub-boundary. This is likely to confirm the situation shown in Fig. 1(c) as the bulk averaged evidence. The crystallite size determined by the above CMWP fitting was 392.4 nm which was nearly comparable with the size of martensite lath

(γ sub-grains in a Type A grain observed in Fig. 1(b)). The microstructure at 1143 K corresponds to the γ memory; though the grain size is as large as that of the prior γ, it contains a high density of sub-boundary. The result of the 1093 K profile was almost identical with those of the 1143 K profile, but the CMWP fitting for the 1223 K profile could not be finished, suggesting that the microstructure was almost the same as that of the reference sample of a well-annealed austenitic steel (or LaB_6 powder) with a very small density of dislocations.

Such a characteristic austenite reversion behavior is quite different from that observed in a bainite steel in which type B grains were dominantly observed. Fig. 4(a) is an example of diffraction intensity change after the completion of austenite transformation in a bainite steel (1.1Cr-0.36C (mass%) [9]), the initial microstructure of which consisted of ferrite and cementite. As seen, the diffraction intensity is found hardly to change with holding at an elevated temperature, i.e., during grain growth. The normalized 200 diffraction profiles for the two steels were compared in Fig. 2(b) revealing that the line-broadening is large only in the case of the tempered martensite (TM) steel specimen at 1143 K immediately after the completion of austenite transformation. This is similar to the distribution of KAM value observed in Fig. 1, which were summarized as the KAM value versus frequency relationship in Fig. 4(c).

In conclusion, the γ reversion occurs through the nucleation competition of type A and B grains. If the type A occurred predominantly, the γ memory would be observed. Hence, the γ memory must be observed in the case of a very slow heating rate for large-scaled products in industrial processing, in which cementite changes to alloy carbides resulting in the poor population of type B nucleation sites. The reversed γ obtained from the type A grains contain a high density of sub-grain boundaries that are the driving force for the growth of type B grains, leading to a recrystallization-like phenomenon. A schematic illustration of this γ memory phenomenon was given in Fig. 10 of ref. 8. Such microstructural evolution can be monitored through *in situ* neutron diffraction providing the bulk verification of the results of surface observations [8, 9].

Neutron diffraction measurements were performed through project # 2015A0129 at MLF J-PARC. This research did not receive any specific grant from funding agencies in the public, commercial, or not-for-profit sectors.

References

[1] S. T. Kimmins and D. J. Gooch: Met. Sci., 17(1983), 519-532.

[2] V. V. Kubackek and V. D. Sadovskiy: Phys. Met. Metallogr., 43(1977), 101-107.

[3] T. Azuma, Y. Tanaka and T. Ishiguro: Tetsu-to Hagané, 76(1990), 783-790.

[4] T. Hara, N. Maruyama, Y. Shinohara, H. Asahi, G. Shigesato, M. Sugiyama and T. Koseki: ISIJ Int., 49(2009), 1792-1800.

[5] S. Watanabe and T. Kunitake: Trans. Iron Steel Inst. Jpn., 16(1976), 28-35.

[6] S. Matsuda and Y. Okamura: Trans. Iron Steel Inst. Jpn., 14(1974), 363-368.

[7] N. Nakada, T. Tsuchiyama, S. Takaki and S. Hashizume: ISIJ Int., 47(2007), 1527-1532.

[8] T. Shinozaki, Y. Tomota, T. Fukino and T. Suzuki: ISIJ Int., 57(2017), in print.

[9] T. Shinozaki, Y. Tomota, T. Fukino and R. Yoda: CAMP ISIJ, 28(2015), 783.

[10] S. Kabra, K. Yan, D.G. Carr, R.P. Harrison, R.J. Dippenaar, M. Reid and K. Liss: Journal of Applied Physics, 113 (6), 063513-1-063513-8, (2013).

[11] M.T. Huchings, P.J. Withers, T.M. Holden and T. Lorentzen, *Introduction to the Characterization of Residual Stress by Neutron Diffraction*, CRC Press, Taylor & Francis, (2005).

[12] T. Ungár and G. Tichy: Phys. Stat. Sol. (a), 171(1999), 425-434.

[13] G. Ribárik, T. Ungár, *Mater. Sci. Eng.*, A528(2010), 112–121.

[14] T. Ungár, L. Balogh, G. Ribárik, *Metall. Mater. Trans.*, A41(2010), 1202-1209.

Figure captions

Fig. 1

EBSD results: (a)-(d): tempered martensite steel, (e)-(h) bainite steel; (a) and (e): 923 K (before reverse transformation), (b) 1148 K and (f) 1078 K (after reverse transformation), (c) and (f) KAM maps of (b) and (f), respectively, and (d) 1173 K and (h) 1153 K (after growth of austenite grains).

Fig. 2

Change in diffraction profile with annealing: (a) heat history; heating rate after 993 K was 0.05 K/s and iso-temperature holding time was 1.2 ks (A_{c1}= 1003 K, A_{c3} = 1088 K), (b) 2D plots for austenite 111 and 200 and ferrite 110 peaks as a function of annealing time (axial direction data) and (c) diffraction profiles collected within 0.6 ks at the latter half stage of isothermal holding at 1143 and 1223 K (axial direction data). Here, red arrows indicate the maximum intensities at 1223 K and the two 200 peaks were magnified to compare clearly.

Fig. 3

Changes in diffraction intensities and FWHMs determined from profiles obtained in the axial direction: (a) changes in relative hkl diffraction intensities with heating after austenite reversion and (b) changes in relative hkl FWHMs.

Fig. 4

Comparison of dissimilar austenite reversion behaviors for the tempered martensite (TM) and bainite steels, in which the hkl intensity just after the completion of reverse transformation was taken as unity: (a) relative diffraction intensity change with heating for the bainite steel, (b) normalized 200 diffraction profiles of the bainite steel and the

TM steel, and (c) distributions of KAM value related to the micrographs shown in Fig. 1(b), (d), (f) and (h).

Figure(s)

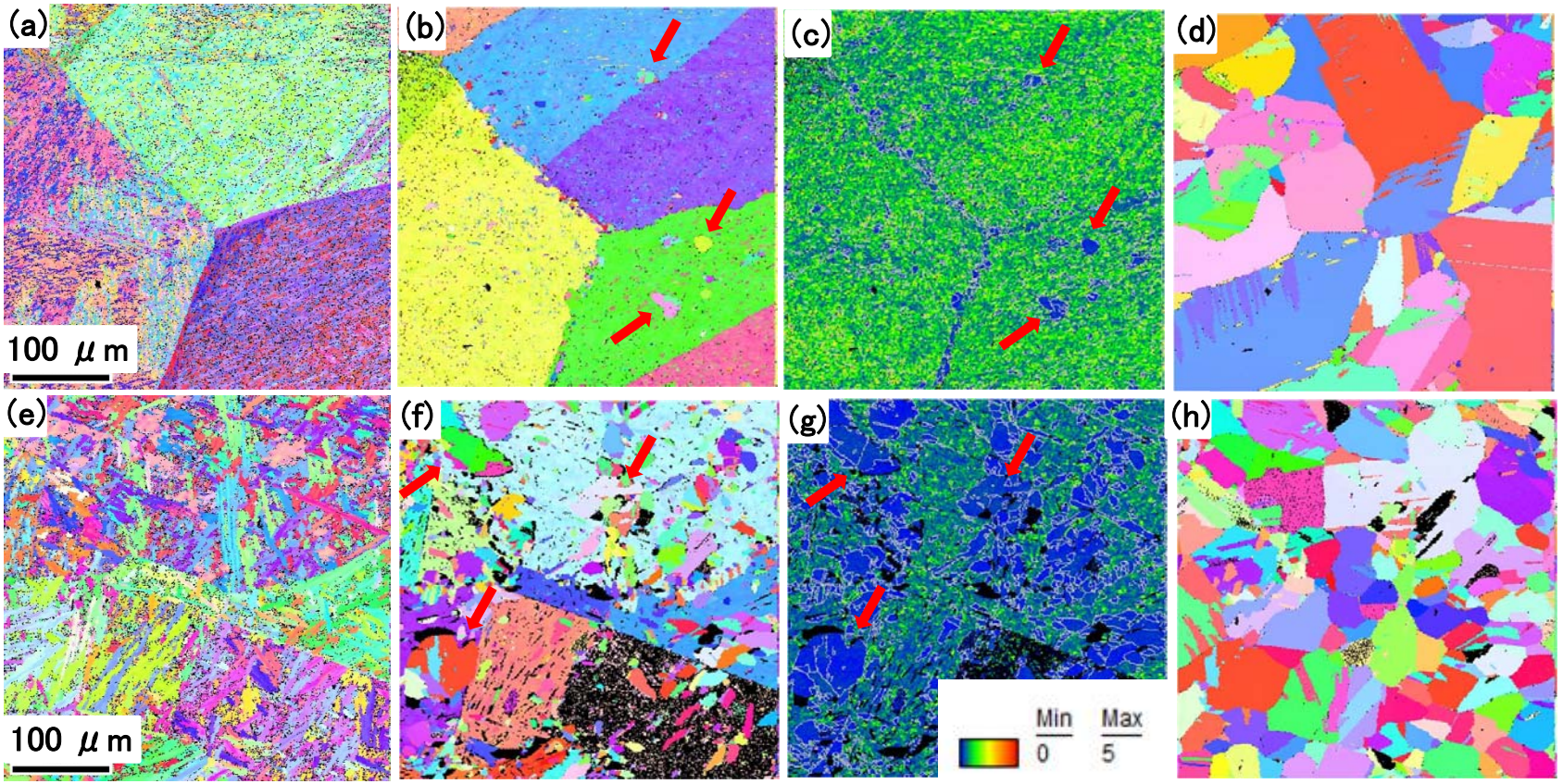

Fig. 1 EBSD results: (a)-(d): tempered martensite steel, (e)-(h) bainite steel; (a) and (e): 923 K (before reverse transformation), (b) 1148 K and (f) 1078 K (after reverse transformation), (c) and (f) KAM maps of (b) and (f), respectively, and (d) 1173 K and (h) 1153 K (after growth of austenite grains).

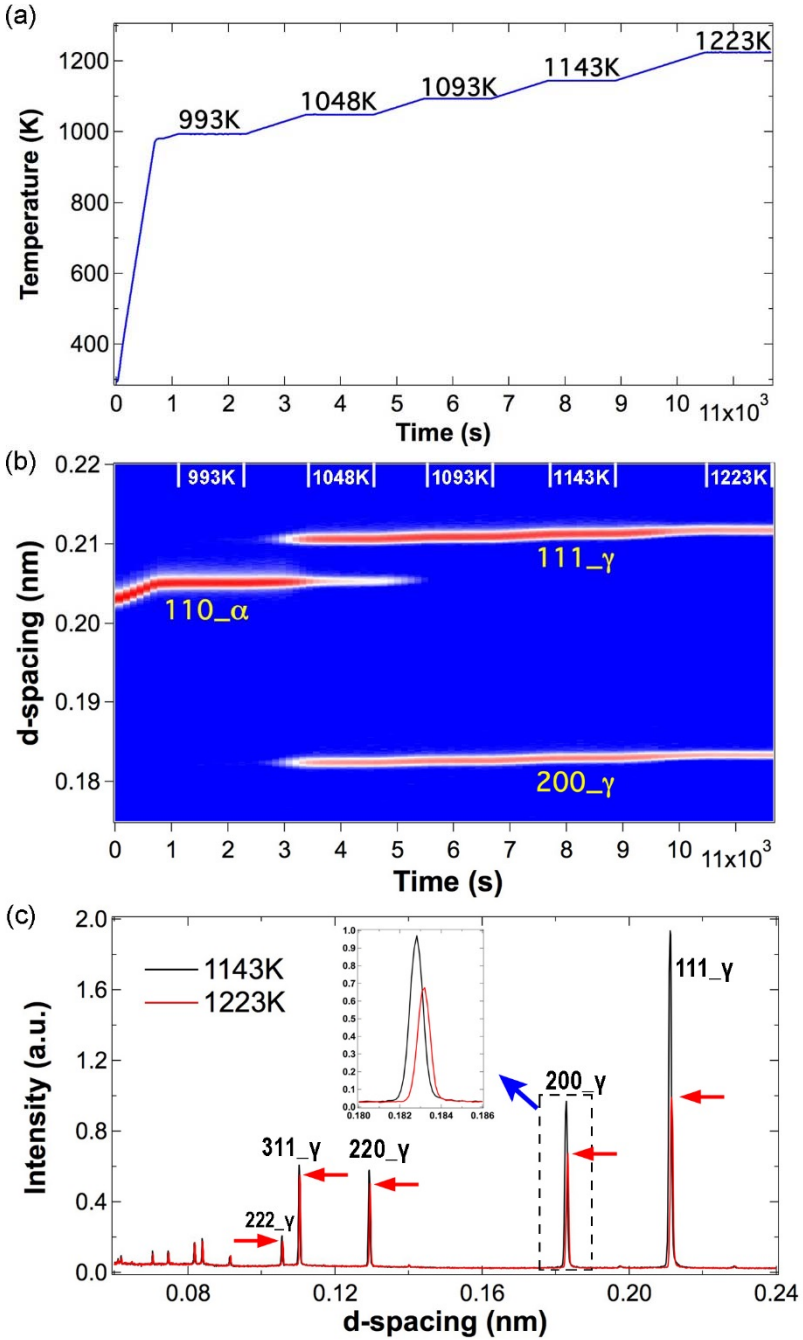

Fig. 2
Change in diffraction profile with annealing: (a) heat history; heating rate after 993 K was 0.05 K/s and iso-temperature holding time was 1.2 ks (A_{c1}= 1003 K, A_{c3} = 1088 K), (b) 2D plots for austenite 111 and 200 and ferrite 110 peaks as a function of annealing time (axial direction data) and (c) diffraction profiles collected within 0.6 ks at the latter half stage of isothermal holding at 1143 and 1223 K (axial direction data). Here, red arrows indicate the maximum intensities at 1223 K and the two 200 peaks were magnified to compare clearly.

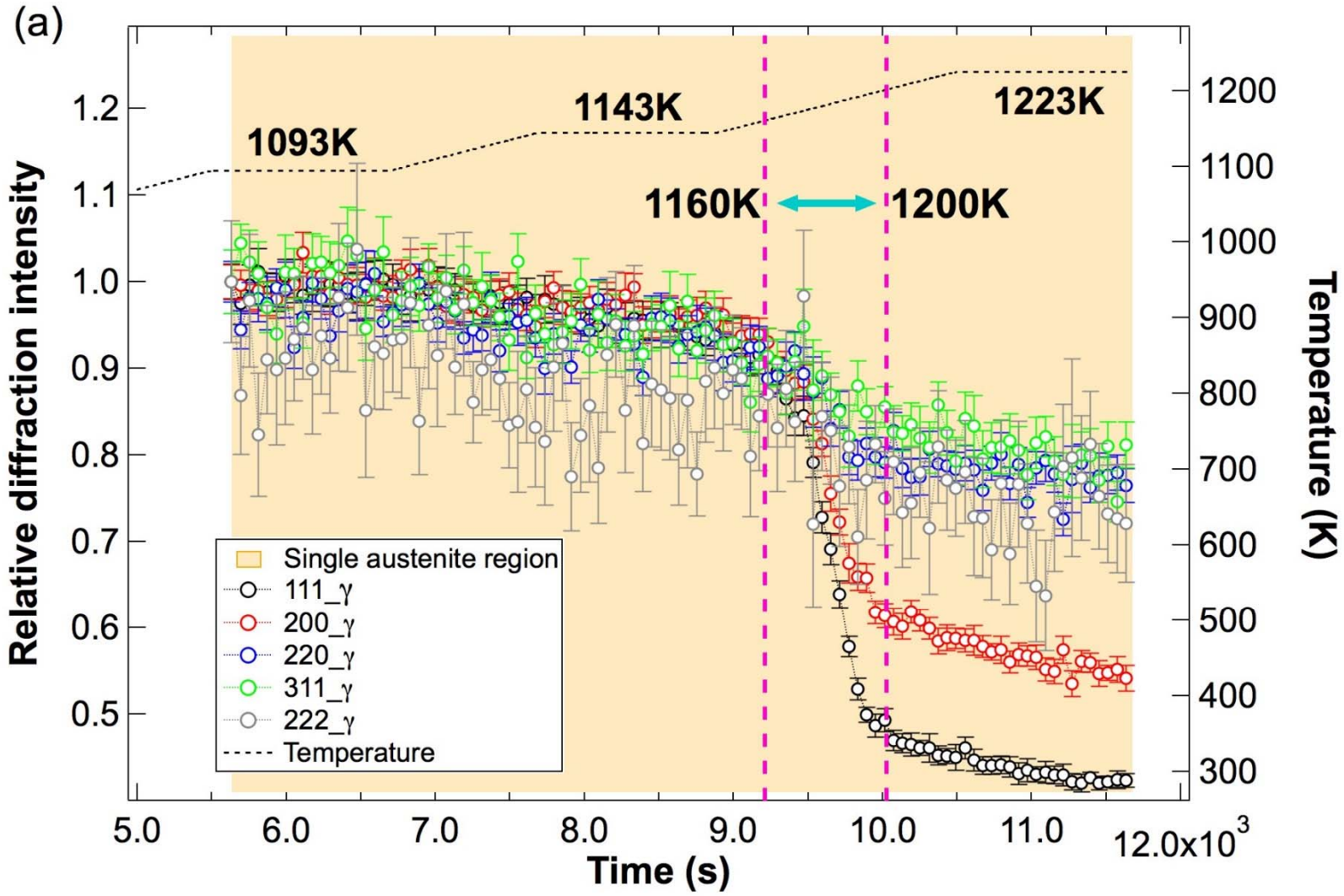

Fig. 3 Changes in diffraction intensities and FWHMs determined from profiles obtained in the axial direction: (a) changes in relative hkl diffraction intensities with heating after austenite reversion and (b) changes in relative hkl FWHMs.

.

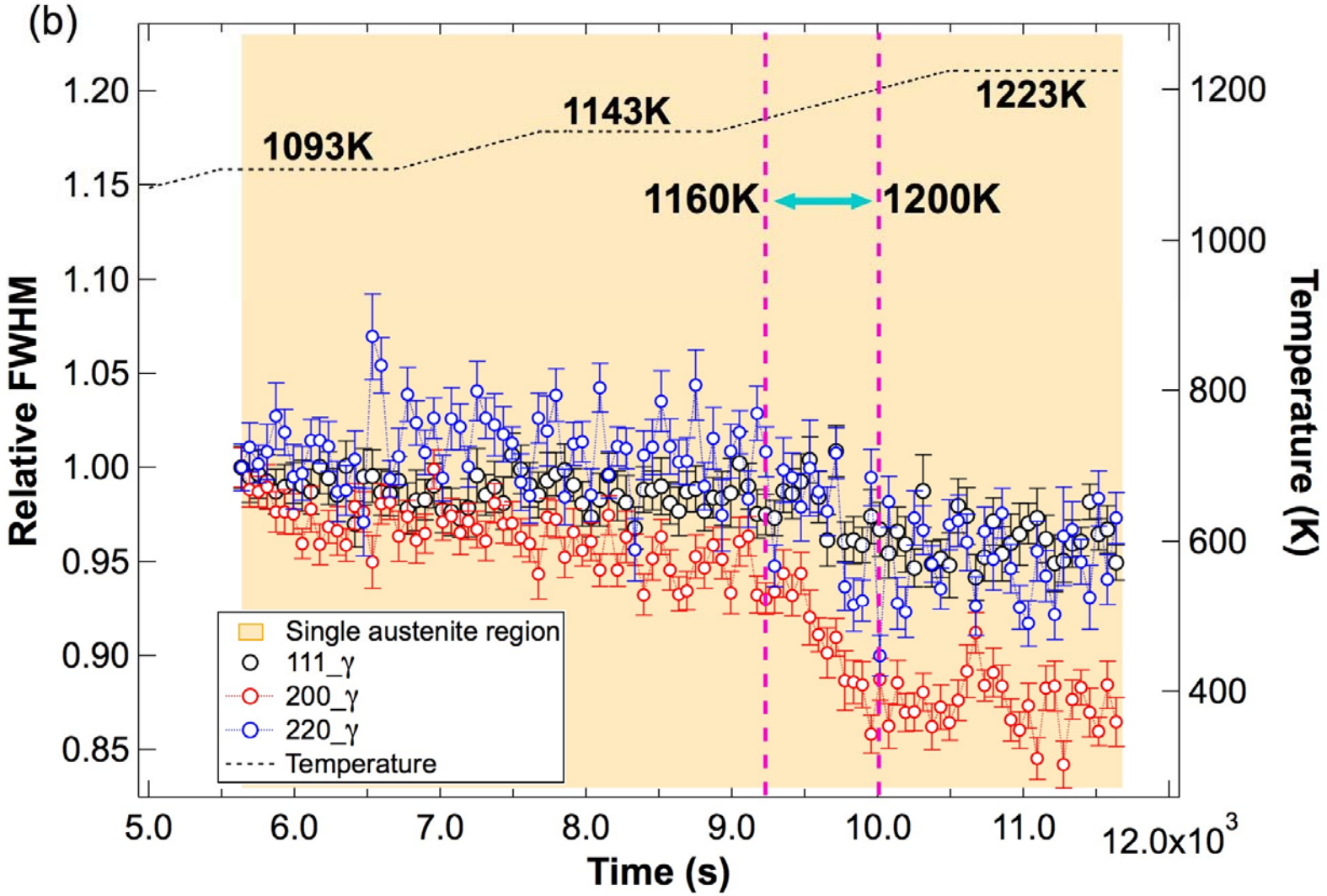
(b)
1093K
1143K
1223K
1160K
1200K
Relative FWHM
Temperature (K)
Time (s)
Single austenite region
111_γ
200_γ
220_γ
Temperature
1.20
1.15
1.10
1.05
1.00
0.95
0.90
0.85
1200
1000
800
600
400
5.0
6.0
7.0
8.0
9.0
10.0
11.0
12.0x10^3

Fig. 3(b)

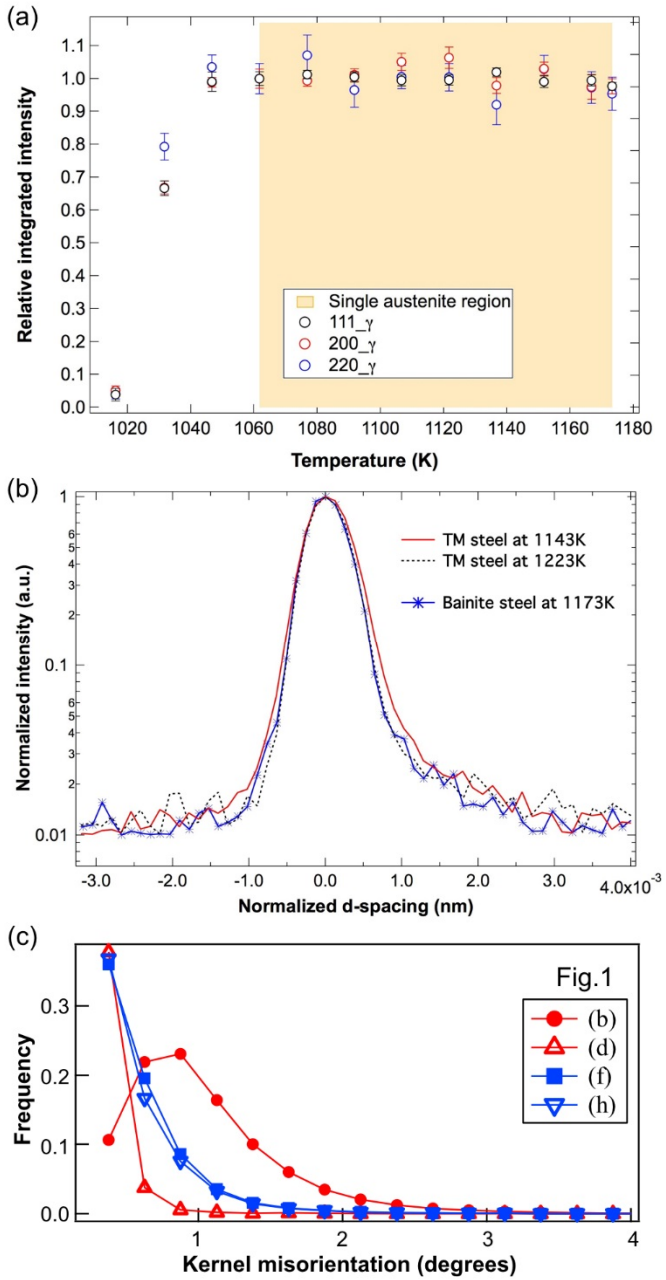

Fig. 4 Comparison of dissimilar austenite reversion behaviors for the tempered martensite (TM) and bainite steels, in which the hkl intensity just after the completion of reverse transformation was taken as unity: (a) relative diffraction intensity change with heating for the bainite steel, (b) normalized 200 diffraction profiles of the bainite steel and the TM steel, and (c) distributions of KAM value related to the micrographs shown in Fig. 1(b), (d), (f) and (h).